Investigations to Improve the Carbon Footprint of Thin Walled Concrete Structures by 3D Printing Prefabricated Elements

Marc-Patrick Pfleger[1](✉), Sebastian Geyer[2], Christian Hölzl[1], and Markus Vill[3]

[1] Building and Design, University of Applied Sciences Vienna, Vienna, Austria
marc-patrick.pfleger@fh-campuswien.ac.at
[2] High Tech Manufacturing, University of Applied Sciences Vienna, Vienna, Austria
[3] Head of Competence Center for Building and Design, University of Applied Sciences Vienna, Vienna, Austria

Abstract. Additive Manufacturing - AM processes are gaining acceptance in many industries due to their unique design freedom. New design approaches such as topology optimization (TO) and structural optimization using lattice structures are possible. Pilot projects in the housing industry show that possible applications, in this case concrete AM, are also conceivable in the context of construction processes. This paper deals with the production of thin-walled concrete structures and shows material-related reduction potentials compared to conventional prefabricated concrete components. To this end, various extrudable high-performance mortars, some with fiber admixtures, have been developed and an appropriate standardised test specimen has been designed. On the basis of numerous material tests, it was possible to derive significant statements about the application limits of the developed materials, which are fundamental for the design of topo-logically optimised cross-sections of concrete components. The aim of this research project in the field of concrete AM is to produce segmentally built flexural beams and to investigate their load-bearing capacity. The test beams consist of several segments, each with a concrete formulation and a 3D design adapted to its calculated stresses. The segments themselves are manufactured without any classical reinforcement elements and are joined together after the manufacturing process with the application of prestressing with or without subsequent bonding. The segments can also be CO_2 cured in an accelerated process prior to prestressing to further improve the material properties and to further reduce the environmental footprint through CO_2 storage.

Keywords: Topology Optimization · Concrete AM · CO_2 Curing

1 Introduction

Additive manufacturing processes with concrete are already being used experimentally in the first building and civil engineering projects. Examples include some smaller buildings or additions to existing structures [1]. Only a few cases of printed parts with higher

A. Jędrzejewska et al. (Eds.): SynerCrete 2023, RILEM Bookseries 44, pp. 653–664, 2023.
https://doi.org/10.1007/978-3-031-33187-9_60

flexural strength are known, e.g. (segmental) bridges with short spans [2]. The reason for this is mostly due to the greater difficulty in inserting classical reinforcing elements during the printing process. Therefore, a first approach was to further investigate the use of tensile reinforcement elements that can be inserted into the cross-section afterwards.

2 State of the Art and Research Objective

AM processes are opening up completely new production possibilities in various industries. Prototypes, one-offs and small series can be produced in a cost and material efficient way. Numerous research and development projects are being carried out internationally in the field of additive manufacturing [3–7]. However, a closer analysis shows that the majority of solid building components, especially walls, are printed from concrete or mortar, with no material savings due to the lack of dissolution of the structures. Particularly with regard to minimising the environmental impact of concrete, at least 8% of man-made CO_2 emissions are due to cement production [8], a targeted material application according to static requirements would be desirable. Thin-walled, unfilled, printed concrete elements have not yet been used in most pilot projects for AM of buildings.

The overall aim of the research was to produce topologically optimised concrete beams capable of withstanding flexural stresses through the incorporation of unbonded tendons. The AM process itself requires a material that can be applied in layers to build objects. It is therefore not possible to integrate conventional, slack rebar into a cross-section in such an automated process. Specially developed concretes, with and without fibre admixtures, and guided prestressing elements have been used to produce components designed for flexural loading. A number of questions have been raised about the behaviour of the material on printed concrete objects, e.g. the bonding of the layers at the layer boundaries, the influence on the compressive, shear and tensile strength as a function of the direction of the force, etc. The answers to these questions are given in the following sections. It should be noted that typical test methods on cast prisms, cubes or cylinders provide unsatisfactory results and conclusions on the behaviour of components due to the significantly different manufacturing process.

3 Materials and Methods

Conventional and standardized raw materials were used for the mortar mix. This approach was based on the fact that it is more convenient to estimate the behavior of the material in terms of its strength and durability parameters. Initial tests were carried out using manual temporary equipment to determine workability, possible processing times, curing times and post-processing methods. A selected number of mortar variants were then tested for suitability for automated application using a small, stationary 6-axis robot system (ABB IRB140). A screw pump with reservoir was used to feed the material into the extruder. The tube pressure ranged from 5 to 15 bar, depending on the consistency and composition of the material, particularly in relation to the maximum particle size. The final formulations were based on CEM II B-L, quartz aggregate with a maximum grain size of 0.6–2 mm and microsilica. Superplasticizer and thickener were added to improve the green concrete properties. The use of glass fibers already has an effect on fresh concrete through improved compressibility.

In order to increase the build volume and to be able to produce longitudinal components according to the usual requirements, a track motion system (ABB IRBT2005 Track Motion) was used for the final production line, on which a robot with a larger build space (ABB IRB2600) was mounted (Fig. 1).

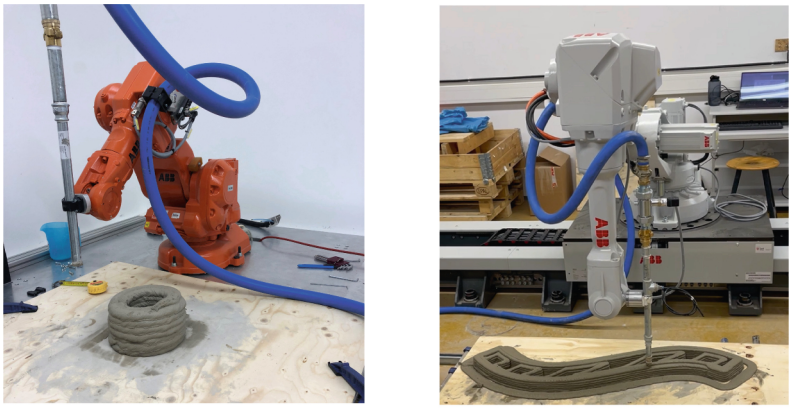

(a) (b)

Fig. 1. The robotic systems used in both (a) the preliminary experiments ABB IRB140 and (b) the final production system with ABB IRB2600 robot and ABB IRBT2005 Track Motion.

In order to homogenize the material flow and the wall thickness of the objects to be produced, a PID pressure control system has been added to the production line via a PLC. A nozzle diameter of approximately 10 mm is used with a maximum grain size of 1 mm. The outer shells of the parts produced are double stranded, which gives cleaner contours to the parts, while the infill consists of a single strand of material, which is sufficient to give the parts the desired inner stiffness. In order to produce concrete AM parts with the robotic system, a variety of different software tools are used, such as CAD, slicer software and machine-specific software for the robotic system (see Sect. 5).

4 Preliminary Experiments

Material development and, in particular, suitable data processing and provisioning for this specific AM process had to be developed from scratch. The necessary know-how was gained through an empirical approach (Fig. 2).

Several material mixtures with sufficient extrudability were tested for compressive and tensile strength. Obviously, fibre-reinforced mortars show better performance in terms of their material specifications compared to mortars without fibres. At the same time, an excessively high fiber content leads to a deterioration in the pumpability or extrudability of the material with the screw pump used [9, 10] (Fig. 3).

The material properties listed in Table 1 are mean values of the test results of 2 series of specimen with and without glass fiber admixture.

(a) (b) (c)

Fig. 2. Preliminary experiments with the ABB IRB140, (a) first try, (b) after adjustment of both speed and layer thickness, (c) fully dried specimen

(a) (b)

Fig. 3. Test setup of the 3 point bending test (a), and fracture surface of a 3D printed test specimen (300 × 120 × 100 mm) made of glass fiber reinforced concrete (b).

Table 1. Mean values of the results of material testing after curing for 10 days

Dimensions [mm]	Glass fibers [mass%]	Hole share [%]	Density [g/cm^2]	Flexural strength [N/mm^2]	Compressive strength [N/mm^2]	Shear strength [N/mm^2]
300 × 120 × 100	0	30	2,09	4,92	46,22	5,36
300 × 120 × 100	0,5	30	2,02	6,44	53,85	7,02

5 Design, Production and Analysis

5.1 Design and Modelling

The basic objective was to produce a bending member with a rectangular profile and integrated cavities, using significantly less material than a comparable conventionally manufactured product. Due to the high mechanical resistances of the material, the cross-section was reduced to an approximately 2–2.5 cm thick frame with stiffening elements

inside the cavity. The stiffening structure also acts as a guide for prestressing elements and does not extend over the full length of each beam segment.

A fully parametric CAD model was initially created in Rhino 7 as a design study. The CAD platform was later changed to SolidWorks and a more refined model was created (Fig. 6a). The model was then exported as an STL and a GCode file was generated in Simplify3D (Fig. 6b) using specific values for layer thickness and extrusion diameter, as well as infill overlap, obtained from preliminary trials. The required thickness of the perimeter lines was achieved by moving the nozzle along the planned path and adding an offset as a second set of paths on the inside of the lines.

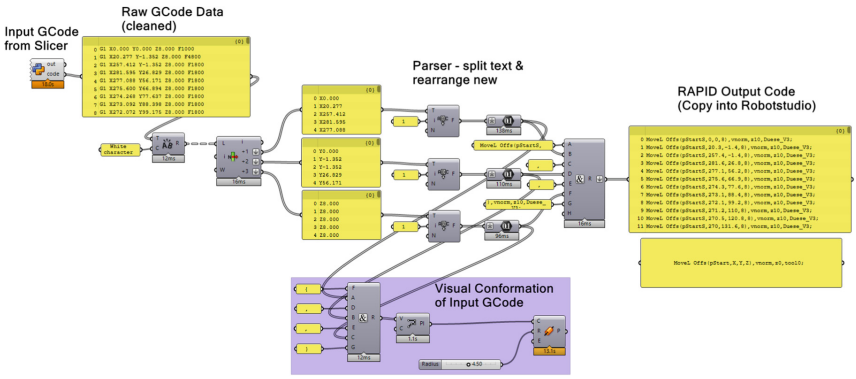

Fig. 4. Developed GCode to RAPID parser.

A bespoke Grasshopper algorithm in the Rhino 7 environment (Fig. 4) was used to parse the X, Y and Z values from the GCode (e.g. G1 X20 Y1 Z8 F1800) into a RobotStudio executable programming language. The resulting GCode point values X, Y and Z were then inserted into the value set MoveL Offs(pStart,X,Y,Z),vnorm,z0,tool0; where all subsequent points were offset from the original point pStartS. All other values G (move), F (speed) and E (E-steps - extruder value) were discarded as they were not needed for this specific purpose. The output of the file parser was visualised in Rhino/Grasshopper (Fig. 6c) to validate the desired shape before the lines of code were copied into the RAPID environment of Robot-Studio.

A more sophisticated tool chain was developed in Grasshopper/Rhino using the RobotComponents program. The ability to use absolute joint values for the motion of both the robot arm and the external axis means that the possible build space of 1 × 6 × 1 m can now be fully utilised. The previously developed file parser was therefore integrated into the workflow of the RobotComponents program, where both the robot arm, the external axis and the build platee were defined (Fig. 5).

A RAPID routine with a defined start and end point and the activation and deactivation of the screw pump via a digital output was developed and simulated in RobotStudio (Fig. 6d). The programme was then uploaded to the robot controller and production of the sections began (Fig. 6e). After curing for 5 days, one of the resulting concrete parts can be seen in Fig. 6(f).

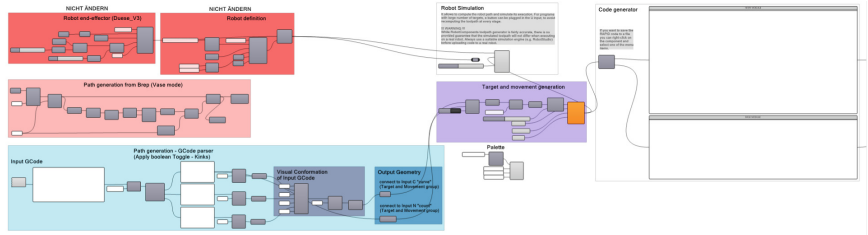

(a)

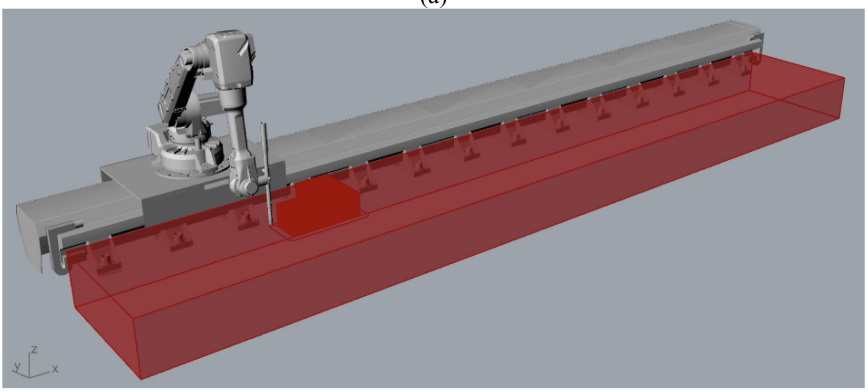

(b)

Fig. 5. Developed RobotComponents toolchain in Grasshopper (a), Visualisation of RobotComponents in Rhino (b)

A comparison of the parametric CAD model with the printed prototype shows production-related deviations, in particular varying wall thicknesses and inaccurate corner areas, Fig. 6(e) and (f). Due to the early stage of the project, production parameters were limited and a cross-sectional shape had to be found that would allow the individual beam segments to be printed upright. This will result in a vertical orientation of the printed layers, with the characteristic groove between the material layers, which can be a potential weakening input for the produced part, oriented perpendicular to the compressive stresses from the tendons, as seen in Fig. 8(b).

5.2 FEM

The cross section produced was designed for manufacturability and is considered a prototype. Structural analysis, in particular FEM simulation, was carried out once the segment structure had been defined and manufactured. Only the outer profile has been used as the stress cross-section. The stiffening infill has not been considered for the analysis under moment loading. The sidewalls have been designed straight in the FEM model due to software-related limitations. The sidewalls of the actually manufactured object have a slight inward curvature to provide additional stability of the green concrete during the printing process. The materials were considered in the modelling according to their design characteristics: C50/60 for the additively manufactured sections as well as for the subsequent top concrete and B550 (yield strength of 550 N/mm^2) for the inserted

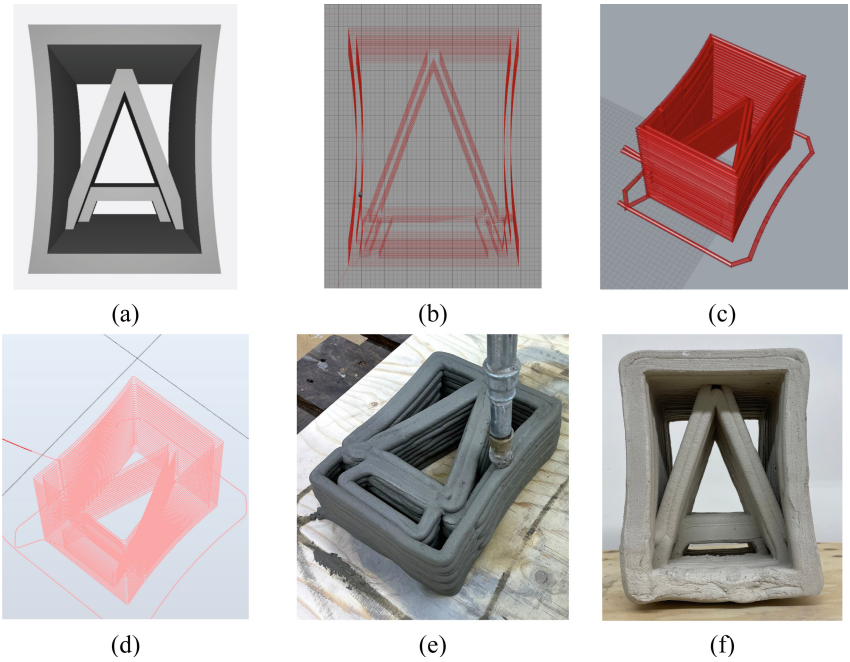

Fig. 6. Overview of the AM workflow for concrete printing, (a) CAD model, (b) GCode visualization, (c) Grasshopper file parser visualization, (d) RobotStudio simulation, (e) AM process, (f) finished part.

reinforcement. The result of the INCA 2 stress-strain analysis is shown in Fig. 7 for two load cases (dead load, ultimate limit state).

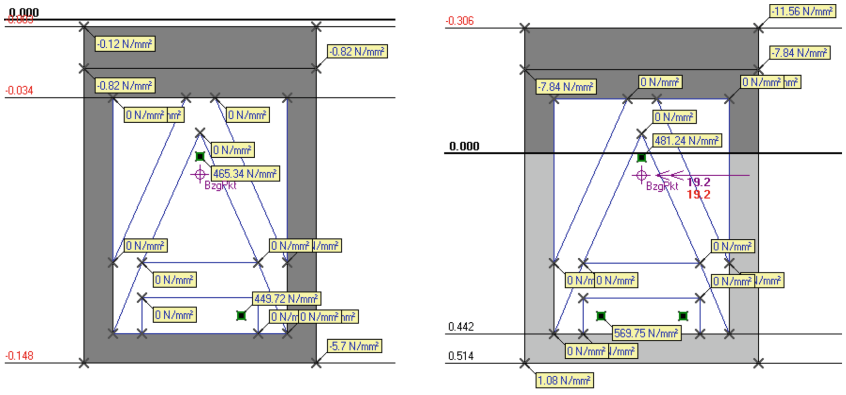

(a) (b)

Fig. 7. Stress-strain analysis in INCA 2 of the prestressed cross-section in the dead-weight case (a) and under load until the steel reinforcement reaches plasticity (b).

The analyses show that the high compressive strength of the printed concrete cannot be efficiently utilized due to the low reinforcement ratio and strength. Nevertheless, the deflection behavior of the beam without additional strengthening measures was investigated and compared with the FEM model. This was necessary to investigate the beam's behavior in the event of cracking in the absence of shear reinforcement.

5.3 Manufacturing

For the production of the modelled beam segments, a mortar recipe without fibre admixture was used in the first approach. As can be seen in Figs. 8(a) and 8(b), the individual cross-section segments have slightly different wall thicknesses due to the different material consistencies of the individual mixing batches.

(a) (b) (c)

Fig. 8. (a) Cross section segment while printing, (b) assembling with mortar joints for uniform force distribution of the individual segments and (c) installation of the anchor plates.

A total of 14 segments were fabricated and assembled into a test beam of approximately 250 cm in length, including the mortar joints. The mortar was used to distribute the forces as evenly as possible between the segments and to avoid stress peaks and point loads that could potentially lead to cracking. The material mix used for this purpose is of the same composition and consistency as the concrete used for the printing. Figure 8(c) shows the installation of the anchor plates, which were subjected to a light compressive load on the beam shortly after assembly to ensure that all component joints were tightly sealed. At the same time, a 3.5 cm wet-on-wet top layer of concrete was poured to provide a uniform static effect and to stabilize the individual beam segments. After the concrete and mortar had set for 28 days, the tendons were prestressed to over 440 N/mm^2, which is approximately 80% of their yield strength.

5.4 Cross-Section Test

The test rig used consisted of a rigid steel beam structure with small deformations in relation to the intended range of test forces. Tilting bearings and load distribution plates for force transmission ensured that the specimen was deformed without restraint. The force from the hydraulic cylinder was transmitted through the horizontal beam to two load application points, each at one third of the beam length, Fig. 9(a).

(a) (b)

Fig. 9. Structural testing in a 4-point bending test with (a) monitoring and documentation of the load-deformation behavior, as well as (b) the crack formation in the joint areas caused by the elastic strain and plasticization of the tendons.

As the load increased, flexural cracks began to form from the center of the beam. As expected, cracking was particularly evident in the area of the mortar joints of the beam segments due to the reduced adhesive strength of the grout on the already hardened printed cross-section. Figure 9(b) shows an example of how flexural cracks were always formed directly at the contact surface between the grout and the beam segment.

The load-deformation of the beam showed an elastic behavior even when the force was reapplied limited by the yield strength of the tendons. Further increases in load results in permanent deflection of the member, although the permanent deformation of the system as shown in Table 2 can be explained by slippage of the non-bonded prestressing. During load application, only a single crack was detected due to the increasing deflection. The corresponding crack width is shown in Table 2 (Fig. 10).

Table 2. Measured force, deformation and crack width of the test beam.

Load stage	Force [kN]	Deflection (loading) [mm]	Crack width [mm]	Deflection (unloading) [mm]
1	0	0	0	0,3
2	4,9	2,1	0,5	2,4
3	9,8	2,8	1,0	3,2
4	12,25	3,6	1,8	3,9
5	14,97	4,1	2,6	4,1

5.5 Ecologic Evaluation and Forced Carbonation

The printed beam segments have a maximum cross-sectional area (referring to the fully stiffened area including the reinforcement guides) of approximately 0.0315 m^2.

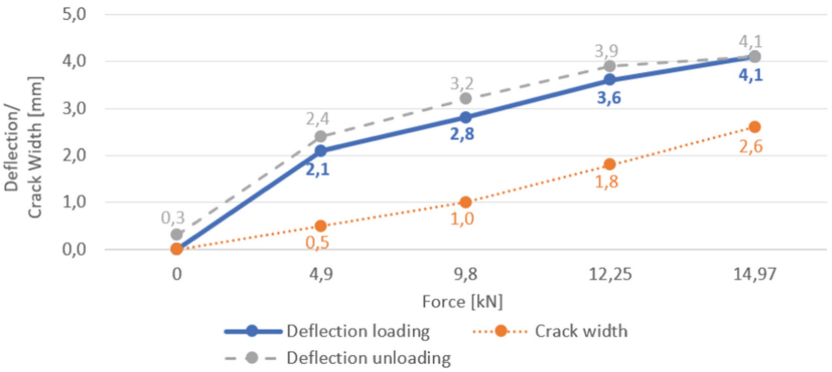

Fig. 10. Load-deflection diagram of the test beam according to values shown in Table 2.

In comparison, a solid section with the same external dimensions has a sectional area of 0.057 m^2. This means that by reducing the infill of the cross-section, only 55% of the concrete mass is required to produce the shown beam element, although a printable mortar recipe has higher cement content than conventional mixtures. The slender cross-section design results in an increased surface area compared to a conventional beam. This provides ideal conditions for using the carbon storage potential of the prefabricated concrete elements. The absence of embedded reinforcement is advantageous because it allows to use a forced carbonation process to store a maximum of CO_2 in short time, without the risk of steel corrosion.

To assess the amount of CO_2 absorbed, a sample of the test beam was placed in a carbonation chamber for 45 h recording the amount of CO_2 consumed. The carbonation depth was then checked conventionally by using phenolphthalein (Fig. 11).

(a) (b)

Fig. 11. 3D printed cross section after storage for (a) 12h in the carbonation chamber and (b) final carbonation state after 45h of CO_2 exposure.

After 45 h of storage in the carbonation chamber, 330 g of CO_2 has been absorbed by the sample, which weighs approximately 4150 g. When the sample was removed from

the chamber, complete carbonation was not observed. However, with a CO_2 absorption of approximately 8% of the sample's mass, a considerable storage capacity is possible.

6 Conclusion and Outlook

The study shows that high material strength and sufficient properties can be achieved with 3D printed concrete parts, although inhomogeneities theoretically occur due to the manufacturing process. In the present case, the compressive strength of the concrete can only be used to a limited extent due to insufficient reinforcement ratio. Therefore, an additional external prestressing of higher strength is to be installed and a compression failure of the concrete due to flexural stress is to be induced. The integration of reinforcement elements to provide an improved load-bearing behaviour concerning shear forces will be part of further cross-section designs.

The transition from segmental to axial production of beams will be developed and established in the future. This approach can generally reduce or even eliminate the number of component joints. In addition, bondless prestressing is to be replaced by bonded tendons in order to achieve an improved and distributed crack pattern. Nevertheless, the research approaches for material-efficient and thus more ecological production of load-bearing concrete components can be demonstrated by innovative production methods.

The authors would like to thank the Municipal Department 23 of the City of Vienna, Austria for providing funding for this research project.

References

1. Young, R.: World's 1st Printed Neighbourhood Being Built in Mexico. https://www.wbur.org/hereandnow/2020/02/06/worlds-first-3d-printed-neighborhood-mexico
2. Eindhoven University of Technology. https://www.tue.nl/en/news-and-events/news-overview/01-01-1970-nijmegen-has-the-longest-3d-printed-concrete-bicycle-bridge-in-the-world/
3. Paolini, A., Kollmannsberger, S., Rank, E.: Additive manufacturing in construction: A review on processes, applications and digital planning methods. Addit. Manufact. **30** (2019)
4. Wu, P., Wang, J., Wang, X.: A critical review of the use of 3-D printing in the construction industry. Automat. Construct. **68**, 21–31 (2016)
5. Butler-Millsaps, B.: WASP Makes Progress on House 3D Printing With Modular Printed Reinforced Concrete Beams. https://3dprint.com/88467/waspmakes-progress-on-house-3d-printing-with-modular-printed-reinforced-concretebeams/
6. Martens, P., Mathot, M., Bos, F., Coenders, J.: Optimising 3D printed concrete structures using topology optimisation. In: Hordijk, D.A., Luković, M. (eds.) High Tech Concrete: Where Technology and Engineering Meet, pp. 301–309. Springer, Cham (2018). https://doi.org/10.1007/978-3-319-59471-2_37
7. Buswell, R., Soar, R., Gibb, A., Thorpe, A.: Freeform construction: mega-scale rapid manufacturing for construction. Automat. Construct. **16**, 224–231 (2007)
8. Mauschitz, G.: Emmissionen aus Anlagen der österreichischen Zementindustrie, Berichtsjahr 2021. Technical University of Vienna (2022)

9. Marchon, D., Kawashima, S., Bessaies-Bey, H., Mantellato, S., Ng, S.: Hydration and rheology control of concrete for digital fabrication: Potential admixtures and cement chemistry. Cem. Concr. Res. **112**, 96–110 (2018)
10. Öcel, C., Yücel, K.T.: Effect of cement content, fibers, chemical admixtures and aggregate shape on rheological parameters of pumping concrete. Arab. J. Sci. Eng. **28**, 1059–1074 (2013)